Acta Neuropathologica
Communications

Open Access

PS1/gamma-secretase acts as rogue chaperone of glutamate transporter EAAT2/ GLT-1 in Alzheimer's disease

Florian Perrin[1*†], Lauren C. Anderson[1†], Shane P. C. Mitchell[1], Priyanka Sinha[1], Yuliia Turchyna[1], Masato Maesako[1], Mei C. Q. Houser[1], Can Zhang[1,2], Steven L. Wagner[3,4], Rudolph E. Tanzi[1,2] and Oksana Berezovska[1*]

Abstract

The recently discovered interaction between presenilin 1 (PS1), a subunit of γ-secretase involved in amyloid-β (Aβ) peptide production, and GLT-1, the major brain glutamate transporter (EAAT2 in the human), may link two pathological aspects of Alzheimer's disease: abnormal Aβ occurrence and neuronal network hyperactivity. In the current study, we employed a FRET-based fluorescence lifetime imaging microscopy (FLIM) to characterize the PS1/GLT-1 interaction in brain tissue from sporadic AD (sAD) patients. sAD brains showed significantly less PS1/GLT-1 interaction than those with frontotemporal lobar degeneration or non-demented controls. Familial AD (fAD) PS1 mutations, inducing a "closed" PS1 conformation similar to that in sAD brain, and gamma-secretase modulators (GSMs), inducing a "relaxed" conformation, respectively reduced and increased the interaction. Furthermore, PS1 influences GLT-1 cell surface expression and homomultimer formation, acting as a chaperone but not affecting GLT-1 stability. The diminished PS1/GLT-1 interaction suggests that these functions may not work properly in AD.

Keywords Alzheimer's disease, Presenilin 1, EAAT2, GLT-1, Glutamate transport, Hyperactivity, Gamma-secretase, Chaperone

Introduction

One of the hallmarks of the neurodegenerative disease Alzheimer's disease (AD) is the formation of extracellular amyloid-beta (Aβ) plaques. Presenilin 1 (PS1), a catalytic subunit of γ-secretase, has been established as a critical player in the development of AD pathology in part because PS1 is responsible for the cut that determines the length of the amyloid β (Aβ) peptides [14, 73]. Familial AD (fAD) mutations in the PS1 protein result in pathogenic conformational changes that correlate with an increased Aβ 42/40 ratio and increased plaque formation [5, 8, 67]. In the search for potential interactors of PS1, we previously identified a novel interaction between the PS1 and glutamate transporter 1 (GLT-1 in rodents, excitatory amino acid transporter 2, EAAT2, in humans), the major glutamate transporter in the brain [81].

†$Florian Perrin and Lauren C. Anderson have equally contributed to this work.

*Correspondence:
Florian Perrin
fperrin@mgh.harvard.edu
Oksana Berezovska
oberezovska@mgh.harvard.edu
[1] Department of Neurology, MassGeneral Institute for Neurodegenerative Disease, Massachusetts General Hospital, Harvard Medical School, Charlestown, MA 02129, USA
[2] McCance Center for Brain Health, Massachusetts General Hospital, Boston, MA, USA
[3] Department of Neurosciences, University of California San Diego, La Jolla, CA 92093, USA
[4] VA San Diego Healthcare System, La Jolla, CA 92161, USA

Perrin *et al. Acta Neuropathologica Communications*   (2024) 12:166

Page 2 of 17

Hyperactivity, epileptic seizures, and impaired glutamate transport occur early in AD pathology prior to most other known changes, including cognitive decline [7, 19, 42, 57, 69]. In fact, alterations in glutamate transporter expression precedes amyloid plaque formation in AD mouse models [9, 24, 50] and glutamate dysregulation occurs prior to and positively correlates with cognitive decline in humans [7, 15, 63]. EAAT2/GLT-1 is responsible for a majority of glutamate uptake from synapses [59, 60] and has been implicated both in mouse models and in humans as having a large role in glutamate dysfunction [23, 46, 48, 52, 76, 83]. Notably, upregulation of GLT-1 in an AD mouse model alleviated cognitive deficits [16], and higher GLT-1 expression was observed in brains from individuals with AD pathology but not dementia compared to those of individuals with AD pathology and dementia [32]. However, the physiological modulators of the aberrant glutamate uptake in AD, and what might be causing GLT-1 to become dysregulated, are not yet well understood.

We have recently reported that GLT-1 directly binds and interacts with PS1/γ-secretase [51, 81] and have hypothesized that the PS1 and GLT-1 interaction is a functional one that may become dysregulated in AD. Previous reports have linked PS1/amyloid pathology to glutamate activity: AD patients, particularly those with mutations in PS1, have a higher incident of epileptiform activity [12, 49]. Moreover, patients with childhood epilepsy, when examined 50 years later, exhibited an increase in amyloid load, a risk factor for developing AD later in life [29]. PS1 deficient neurons had a significant decrease in glutamate uptake [77] and GLT-1 deficiency in an APP/PS1 fAD mouse model increased memory deficits as well as the $A\beta_{42}/A\beta_{40}$ ratio [47]. Treatment with amyloid-beta peptide $A\beta_{1-40}$ decreased GLT-1 uptake capacity in primary rat astrocyte cultures [43] and treatment with $A\beta_{1-42}$ reduced GLT-1 cell surface expression in mouse brain hippocampal slices [61]. Therefore, the interaction between PS1 and GLT-1 that we identified [81] may be the link between two major pathological aspects of AD and could provide a potential novel therapeutic target for AD.

The current studies investigated the molecular link between PS1 and GLT-1 by examining its interaction in sporadic AD (sAD), FTLD, and Control human brains. Additionally, we assessed the impact of changes in PS1 conformation due to fAD PS1 mutations and γ-secretase modulators (GSMs) on the interaction, and explored PS1 effect on GLT-1 cell surface expression, multimerization, and stability. We found increased GLT-1 aggregation and disrupted PS1/GLT-1 interaction in sAD human brain, and revealed that PS1 potentiates GLT-1 cell surface expression and multimerization. We show the interaction is affected in vitro by PS1 conformational changes in a way that may affect GLT-1's normal cellular functioning in the brain.

Material and methods

Human brain tissue

Human brains from neuropathologically verified AD or Frontotemporal lobar degeneration (FTLD) cases were obtained from the brain bank of the Alzheimer's Disease Research Center (ADRC) at Massachusetts General Hospital. Control cases were non-demented individuals who did not meet pathological diagnostic criteria of AD, FTLD or other neurodegenerative diseases (Supplementary Tables 1 and 2). All the subjects or their next of kin gave informed consent for the brain donation. Hippocampal and frontal cortex sections were used for immunohistochemistry; frontal cortex samples were used for Western blotting/immunoprecipitation. This article does not contain any studies with human participants or animals performed by any of the authors.

Cell cultures and transfection

Chinese hamster ovary (CHO) cells were maintained in OPTI MEM medium supplemented with 5% FBS in a 37 °C CO_2 incubator. Human embryonic kidney (HEK) cells in which PS1 and PS2 are knocked down (HEK PS DKO) were kindly provided by Dr. Dennis Selkoe, BHW, Boston, MA, and were maintained in DMEM supplemented with 5% FBS, 1% GlutaMax and 1% Pen/Strep mix (Life Technologies, Carlsbad, CA) in a 37 °C CO_2 incubator. Lipofectamine 3000 (Life Technologies, Carlsbad, CA) was used for transient transfection according to the manufacturer's instructions.

HEK PS DKO and HEK wt were transduced with lentivirus expressing GLT-1 GFP and selected with 10 μg/mL of puromycin to generate HEK PS DKO GLT-1 and HEK wt GLT-1 stable cell lines, respectively.

Plasmid constructs

Plasmids encoding PS1wt and PS1 fAD were cloned into pcDNA3.1 vector (Addgene). The GLT-1 encoding sequence was subcloned into pcDNA^{TM}6 V5 Myc (ThermoScientific). The GFP sequence cloned in pcDNA3.1 was used as negative control for all experiments, except for flow cytometry where pcDNA3.1 empty vector was used and referred to as Mock. Lentivirus production used packaging plasmids psPAX2 and pMD2.G (Addgene), and a third vector pLenti-SLC1A2-C-mGFP-P2A-Puro (Origene).

Perrin *et al. Acta Neuropathologica Communications*   (2024) 12:166

Page 3 of 17

Drug treatments

In the experiments using γ-secretase modulators (GSMs), cells were treated with 20 nM GSM15606 [55], 3 µM GSM36 [71] or dimethyl sulfoxide (DMSO) vehicle control for 16 h. GLT-1 selective inhibitors, DHK (dihydrokainate) and WAY213613 were obtained from Tocris.

Immunocytochemistry (ICC) and Immunohistochemistry (IHC)

PFA-fixed brain tissue was sectioned into 50 µm-thick sections on a Leica freezing microtome (Leica SM 2000R, Bannockburn, IL) and used for IHC immunostaining. For ICC, in vitro cultured cells were washed twice with Dulbecco's Phosphate Buffered Saline without Calcium Chloride or Magnesium Chloride (PBS; ThermoScientific, Waltham, MA) and fixed by 15-min incubation with 4% PFA. Following the fixation, free-floating brain sections or cells were permeabilized using 0.1% TX-100 in a 1.5% normal donkey serum (NDS; Jackson ImmunoResearch labs, West Grove, PA) blocking solution for 1 h. After three 5 min washes in PBS, samples were incubated overnight with respective primary antibodies in 1.5% NDS. Excess primary antibodies were washed off with three 5 min washes in PBS and the corresponding Alexa Fluor 488- or Cy3-conjugated secondary antibodies (1:500) were applied for 1 h at room temperature. Cells and tissue were then washed three additional times in PBS. Cells were coverslipped with VectaShield mounting medium (Vector Laboratories, Inc., Burlingame, CA) and brain sections were mounted onto microscope slides and coverslipped with VectaShield.

Antibodies

The following primary antibodies were used: guinea pig anti-GLT-1 (AB1783, EMD Millipore, Temecula, CA) and rabbit anti-GLT-1 (ab41621, Abcam, Cambridge, MA), both targeting C-term region; rabbit nGLT-1 targeting N-term [11] (kindly provided by our collaborator, Dr. Rosenberg, BCH, Boston), rabbit anti-GLT-1 (NBP120136, Novusbio) undisclosed epitope; rabbit anti-PS1 raised against a.a.263–378 of PS1 (S182, Sigma-Aldrich, St. Louis, MO); mouse anti-PS1 raised against N-term (Biolegends, 823,401), mouse anti-β-actin (A2228, Sigma-Aldrich, St. Louis, MO); rabbit anti-PS2 (mAb 9979, Cell Signaling Technology, Danvers, MA); EGFR (ab52894, Abcam, MA); normal rabbit IgG (2728S, Cell Signaling Technology, Danvers, MA). Alexa Fluor 488 (ThermoScientific, Waltham, MA) and Cy3-conjugated secondary antibodies (Jackson ImmunoResearch, West Grove, PA) were applied for the microscopy imaging and IRDye680/800- (Li-COR, Lincoln, NE) labelled ones were used for western blotting.

Fluorescence lifetime imaging microscopy (FLIM)

FLIM assay to monitor relative proximity between fluorescently labeled molecules in intact cells/tissue was conducted as described previously [72, 81]. We measured fluorescence lifetime rather than intensity to determine the Forster resonance energy transfer (FRET) efficiency. Fluorescence lifetime is an intrinsic biophysical property of the fluorophore and, unlike fluorescence intensity, does not depend on the concentration or stoichiometry of the donor and acceptor fluorophores [4, 35]. Briefly, cells were immunostained with anti-GLT-1 CT (1:250) and anti-PS1 (loop) (1:250) antibodies. Corresponding secondary antibodies conjugated with Alexa Fluor 488 (AF488) and Cy3 fluorophores were used as the donor and acceptor, respectively. A sample in which the acceptor antibody was omitted was used as a negative control to record the baseline lifetime ($t1$) of the donor fluorophore. A femtosecond-pulsed Chameleon Ti:Sapphire laser (Coherent Inc., Santa Clara, CA) at 850 nm was used for two-photon fluorescence excitation. AF488 fluorescence was acquired using an emission filter centered at 515/30 nm. The donor fluorophore lifetimes were measured with a high-speed photomultiplier tube (MCP R3809; Hamamatsu, Bridgewater, NJ) and a fast time-correlated single-photon counting acquisition board (SPC-830; Becker & Hickl, Berlin, Germany). The data were analyzed using SPCImage software (Becker and Hickl, Berlin, Germany). The AF488 lifetimes were calculated by fitting raw data to the single-exponential (AF488 negative control) or two-exponential (AF488- and Cy3-double immunostained sample) fluorescence decay curves. t_2 Lifetime values that are shorter than t_1 indicate the presence of the FRET, i.e., less than 5–10 nm distance between the donor and acceptor fluorophores. FRET efficiency was calculated by subtracting the measured lifetime ($t2$) from the baseline lifetime ($t1$), divided by t1, expressed as a percentage (i.e. [(t1-t2)/t1]*100).

For human brain tissue, we used three-component analysis of the fluorescence lifetimes to exclude interference of the non-specific signal from autofluorescence/lipofuscin as previously described [72]. Briefly, the baseline lifetimes of AF488 and autofluorescence were calculated by fitting raw data to two-exponencial decay curves (negative control) to determine the value of t1 (autofluorescence, short lifetime ~ 400 psec) and t2 (A488, long lifetime comparable to that in cells in vitro). Then the brain samples immunostained with AF488 and Cy3-labeled antibodies against GLT-1 (1:250) and PS1 (1:250) were analyzed using three-component analysis. The AF488 donor fluorophore lifetime shortening due to

FRET (t3) was then determined by fixing and removing from the analysis t1 (autofluorescence) and t2 (baseline AF488) [72].

Biotinylation of cell surface proteins

To isolate cell surface proteins, HEK PS DKO cells were transiently transfected with pcDNA3.1-GFP (pc) alone, or co-transfected with GLT-1 and pcDNA3.1-GFP or GLT-1 and PS1. All transfections are at 1:1 ratio. The cells were labelled with biotin using an ABCAM kit according to the manufacturer's instructions (ab206998). Pulled down proteins were analyzed by Western blot.

Immunoprecipitation (IP), western blotting (WB), and native blue PAGE

Flash frozen human brain tissue was lysed in 1% 3-[(3-cholamidopropyl) dimethylammonio]-2-hydroxy-1-propanesulfonate (CHAPSO) in buffer (50 mM (4-(2-hydroxyethyl)-1-piperazineethansefulfonic acid [HEPES], 100 mM NaCl, pH 7.4) with Halt protease and phosphatase inhibitor cocktail (Fisher Scientific, Pittsburg, PA, USA). To homogenize the tissue, it was agitated with a pipette 50 times, agitated with a 27guage needle 10 times, rotated at 4 °C for 1 h and then centrifuged for 15 min at 14,000 g at 4 °C. Total protein in the final supernatants was measured using ThermoScientific Pierce BCA Protein Assay (ThermoScientific, Waltham, MA) following the supplier's protocol. Lysis of freshly dissected mouse brain tissue and harvested cells followed the same protocol. Western blotting was performed on the same day as cell/tissue lysis.

For the IP procedure, 50 μl of Protein G Dynabeads (ThermoScientific, Waltham, MA) was incubated with 5 μg of the respective antibody or normal IgG, as a negative control, for 10 min at room temperature. The beads were then collected using a magnet and washed in 0.02%Tween 20 (Sigma-Aldrich, St. Louis, MO) in PBS using a magnetic tube rack. Aliquots of the supernatant containing equal amount of protein (500ug in 400ul) were then added to the beads and incubated overnight at 4 °C with end-over-end rotation. The beads coupled with the complexes were collected, washed three times with 0.02%Tween and transferred to a new tube. The elution was performed by boiling the samples for 5 min in 30 μl Elution buffer (50 mM Glycine, LDS, and DTT-containing reducing agent buffer [ThermoScientific, Waltham, MA]).

To resolve the proteins from the co-immunoprecipitation, biotinylation and cycloheximide preparations, the samples were loaded on 4–12% Bis–Tris NuPage polyacrylamide gels (ThermoScientific, Waltham, MA) and transferred to nitrocellulose membranes (GE Healthcare Lifesciences, Pittsburgh, PA) using BioRad system.

The detection was performed by immunoblotting with specific primary and corresponding IRdye680/800-conjugated secondary antibodies (1:5000) and the bands were visualized using Odyssey Infrared Imaging System (Li-COR, Lincoln, NE). The quantitative analysis of the respective bands' optical density was performed using ImageStudio Lite Ver 5.2 software.

To stabilize potential GLT-1 dimers/trimers we employed disuccinimidyl suberate (DSS) crosslinking agent. After GLT-1/PS1 transfection, HEK PS DKO cells were washed with Ca^{2+} and Mg^{2+} free PBS (PBS-/-). Crosslinking was performed in PBS-/- using DSS dissolved in DMSO at final concentration of 50 μM for 30 min at room temperature and then quenched with 20 mM glycine. Cells were lysed in 1% NP-40+0.1% Triton-X buffer. Fresh lysates were analyzed by western blotting with GLT-1 antibody.

For Blue Native PAGE, the cells were lysed in native blue buffer, digitonin 5% (Invitrogen) and 100X protease inhibitor (Pierce). For human brain tissue, approximately 20 mg of frozen cortical brain tissue was homogenized in 500 μl of 1×NativePAGE sample buffer with digitonin 5% (Invitrogen). After centrifugation (25,000 g, 1 h at 4 °C) supernatants were collected (30 μg of total protein) and 5% of the sample buffer was added. Protein lysates were separated using the Novex® NativePAGE™ Bis–Tris gel system (Invitrogen). The electrophoresis and transfer were performed as per manufacturer's instructions. Membranes were incubated overnight at 4 °C with anti-GLT-1 primary antibody (ABCAM) at dilutions 1:1,000 and anti-rabbit HRP at 1:5,000. Quantification of the bands was performed with ImageJ using area under the curve method.

Flow cytometry

Flow cytometry analysis was used to characterize cell surface expression of GLT-1. CHO cells were transiently transfected with pcDNA3.1 alone (pc) or co-transfected at 1:1 ratio with GLT-1 and pc or GLT-1 and PS1 to evaluate PS1 effect on cell surface GLT-1. At least 300,000 cells were detached with EDTA, fixed with 2% PFA and incubated with GLT-1 antibody (Novusbio) for 1 h at 4 °C with dilution at 1:100 (in 100 μL of PBS with 5% BSA and 2 μM EDTA) followed by PE-conjugated monoclonal antibody (ABCAM) at 1:500 dilution. "Mock" corresponds to CHO cells without GLT-1 transfected only with pcDNA3.1 empty vector and probed with rabbit IgG Isotype control and PE conjugated antibody.

Labeled cells were analyzed by flow cytometry on MACS Quant VYB flow cytometer (Myltenyi Biotec) using FlowJo V10 software. Alternatively, HEK PS DKO and HEK wt cells stably expressing GLT-1 GFP were used without fixation and permeabilization. GFP-GLT-1

signal was measured in the same number of HEK PS DKO GLT-1 GFP and HEK wt GLT-1 GFP cells expressing either PS1 or pcDNA3.1 (pc). "Mock" corresponds to HEK PS DKO cells without GLT-1 GFP and transfected only with pcDNA3.1 empty vector.

Cycloheximide (CHX) assay

Relative protein stability was estimated using a CHX assay. CHO cells and HEK PS DKO cells were co-transfected at 1:1 ratio with GLT-1 and PS1, empty vector, or eGFP, were treated with 20 µg/ml CHX (Sigma-Aldrich) diluted in growth medium. The cells were collected in 0, 4, 8, 24, 32, 48 h time points following the addition of CHX and lysed in 1% CHAPSO buffer with protease and phosphatase inhibitor cocktail. The extracted proteins were analyzed by western blotting. The intensity of each band was quantified using ImageStudio Lite Ver. 5.2 and normalized to the level of protein at the "0" time point. The data were plotted on a graph, fitted with a one-phase decay curve, and analyzed with a Two-way ANOVA followed by Dunnett's multiple comparisons test, using GraphPad Prism 10 software.

Glutamate uptake assay

Previously published procedures were followed for measuring the uptake of glutamate into cells in culture [11]. HEK PS DKO stably expressing GLT-1 GFP were plated at 0.5×10^5 cells per well in 24-well tissue culture plates. Glutamate uptake experiments were performed 2 days after transfections. Cells are washed twice with sodium (Na) (140 mM) or choline (Ch) (140 mM) buffer, both containing 2.5 mM KCl, 1.2 mM $CaCl_2$, 1.2 mM $MgCl_2$, 1.2 mM K_2HPO_4 and 10 mM glucose, buffered to pH 7.4 with sodium phosphate. L-[^{3}H]-glutamic acid (catalog #NET490250UC, PerkinElmer; specific activity 50.8 Ci/mmol) was added at a final total (radioactive plus non-radioactive) glutamate concentration of 50 µM. To verify the specificity of glutamate uptake by GLT-1, cells were treated with an inhibitor of GLT-1 (DHK, 1 mM) or (WAY213613, 10 µM) and uptake compared with vehicle control. Cells were incubated at 37 °C for 5 min and 10 min; the uptake was terminated by washing cells twice in ice-cold choline buffer containing 1% BSA, and cells were solubilized in 0.1 mM NaOH for 30 min, 0.25 ml/well and lysate then transferred to liquid scintillation vials. Total protein content in lysates was determined by Pierce BCA protein assay (ThermoFisher). Radioactivity was assayed by liquid scintillation counting. In all experiments sodium-dependent uptake was determined by subtracting the values obtained in choline buffer from the values obtained in sodium buffer.

Statistical analysis

Statistical analysis was performed using GraphPad Prism 5 and GraphPad Prism 9 software (La Jolla, CA). All the statistical analysis were stated in the figure's legends. Values were considered significant at $p < 0.05$.

Results

Sporadic AD brains have reduced interaction between PS1 and GLT-1

To test whether the PS1/GLT-1 interaction changes due to sporadic AD (sAD), the PS1/GLT-1 interaction was examined using FLIM in intact brain tissue of control, sAD and frontotemporal lobar degeneration (FTLD) patients. The brain sections were immunostained with anti-GLT-1 (Millipore, 1:250) and anti-PS1 (Sigma-Aldrich, 1:250) antibodies. The randomly selected neuronal cell bodies or "neuron-free" parenchyma containing neurites and astrocytes in the frontal cortex and hippocampus sections were outlined as the regions of interest (ROIs) in PS1/GLT-1 immunostained brain sections. The donor fluorophore lifetimes were measured as an indicator of proximity between the GLT-1 and PS1. The sAD tissue showed significantly less interaction between PS1 and GLT-1, measured by a decrease in FRET efficiency, compared to control or FTLD brains in both neuronal cell body-enriched and parenchyma ROIs (Fig. 1; Kruskal–Wallis ANOVA with Dunn's multiple comparison test). Although the PS1/GLT-1 interaction was different, the pattern of GLT-1 and PS1 immunoreactivity seemed comparable between the control brains and brains of sAD patients despite severe neurodegeneration in the latter (Figure S1a). The specificity of GLT-1 immunoreactivity in neuronal cell bodies in human brain was verified using additional anti-GLT-1 antibody, raised against N-terminus (nGLT-1) [11]. The nGLT-1 antibody recognizes both neuronal and astrocytic GLT-1; and was previously tested on brain sections from GLT-1 KO mice [64]. The strongest GLT-1 immunoreactivity derived from astrocytes and neuronal axons within the brain parenchyma, however occasional neuronal cell bodies also showed GLT-1 positivity (Figure S1b). There was no significant effect of age, post-mortem interval (PMI), Braak stage or sex on the interaction in neuronal cell body-enriched or parenchyma ROIs (Figure S2; Kruskal–Wallis ANOVA with Dunn's multiple comparison test).

To further prove the PS1 and GLT-1 interaction occurs in the human brain, coimmunoprecipitation of the PS1/GLT-1 complexes from human brain lysates was carried out (Figure S3a). The interaction was detected in Control, sAD and FTLD brains. Unlike with the FLIM assay, measurable difference in the amount of PS1 coimmunoprecipitated with GLT-1 was not detected (Figure S3b). This divergence could possibly be due to the higher
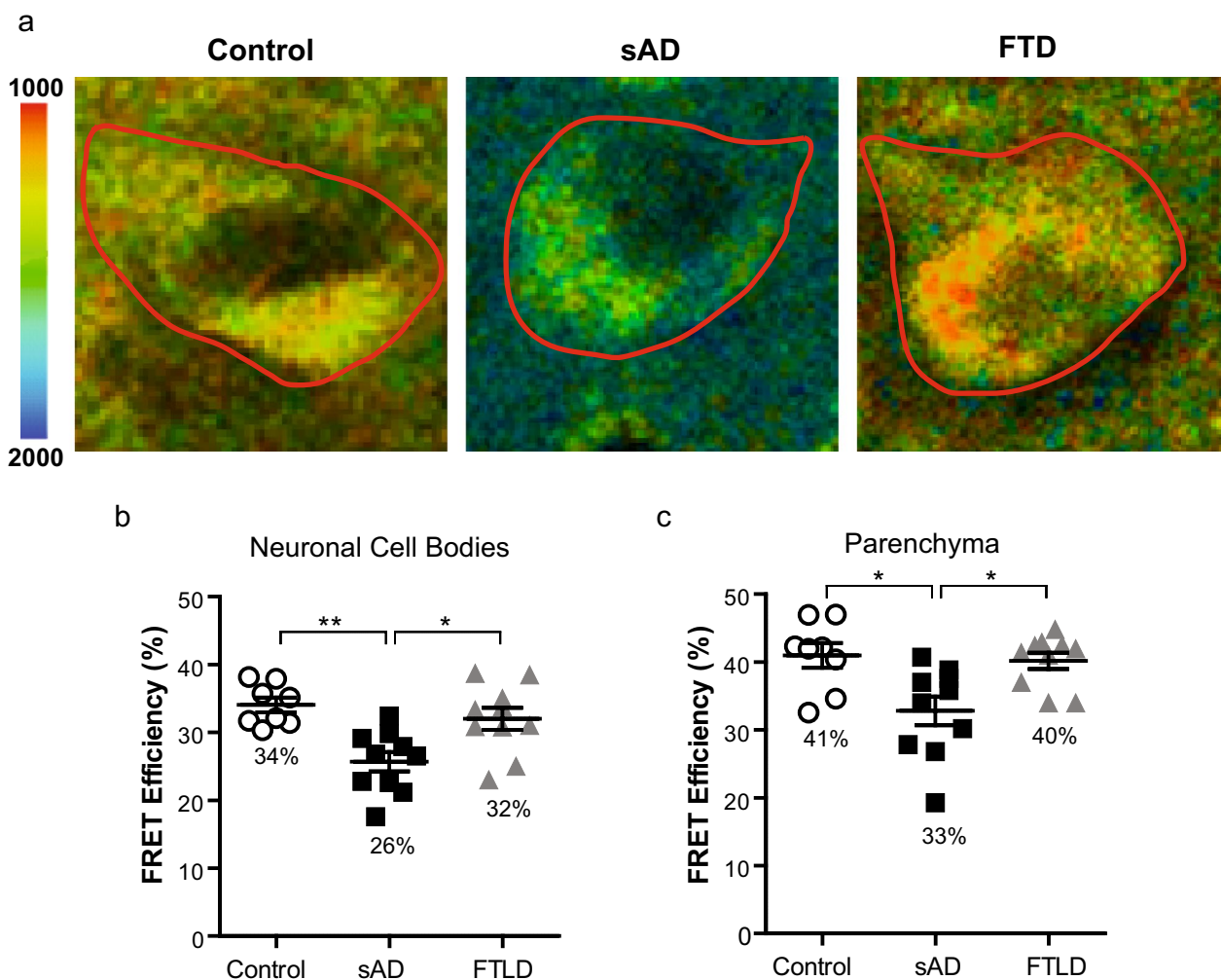
Fig. 1 PS1/GLT-1 interaction changes in sporadic AD **a** Color-coded FLIM images of representative neurons of sAD, control and FTLD brain samples. Donor fluorophore lifetimes in neuronal cell bodies (outlined) and parenchyma (GLT-1 positive synaptic terminals and astrocytes) represent different proximity between fluorophore-tagged PS1 and GLT-1 and thus distance between PS1 and GLT-1 proteins. Colorimetric scale shows fluorescence lifetime in picoseconds (ps). FLIM analysis of the PS1/GLT-1 interaction (%E_{FRET}) in frontal cortex neurons (**b**) and frontal cortex parenchyma (**c**) in human brain. Average %E_{FRET} in sporadic AD (n = 10, ~ 30 neurons per case), non-demented control (n = 8, ~ 30 neurons per case), and FTLD (n = 10, ~ 30 neurons per case) human brain tissue. Bar shows mean ± SEM, *$p < 0.05$, **$p < 0.01$. Kruskal–Wallis ANOVAs with Dunn's multiple comparison test

sensitivity of the cell-by-cell/ROI based FLIM technique, since the latter approach monitors relative proximity between proteins in their native environment without the need of lysis buffer and detergents and can better capture "weak" or more transient interactions.

PS1 conformational state modulates interaction with GLT-1

PS1 has been known to adopt the pathogenic closed conformation in sAD, but not in FTLD, and as a result of fAD PS1 mutations [5, 67, 72]. Alternatively, treatment with NSAIDs or gamma-secretase modulators (GSMs) lead to a more relaxed, open PS1 conformation

[41, 67]. Thus, we wanted to first examine if PS1 pathogenic mutations disrupts the interaction between PS1 and GLT-1. HEK PS DKO cells were transiently co-transfected with GLT-1 and either wildtype or mutant PS1 (Fig. 2c), and the PS1/GLT-1 proximity was evaluated in intact cells by FLIM. Of note, the FLIM assay is not concentration-dependent [34, 36], and FRET efficiency (proximity between PS1 and GLT-1) is not impacted by PS1 wt or fAD expression level. HEK PS DKO co-expressing GLT-1 with PS1 wt or fAD PS1 Δ9, L166P and G384A mutants were stained with Cy3- and AF488-fluorophore labeled antibodies to detect the GLT-1 and PS1, respectively (Fig. 2a top two panels).
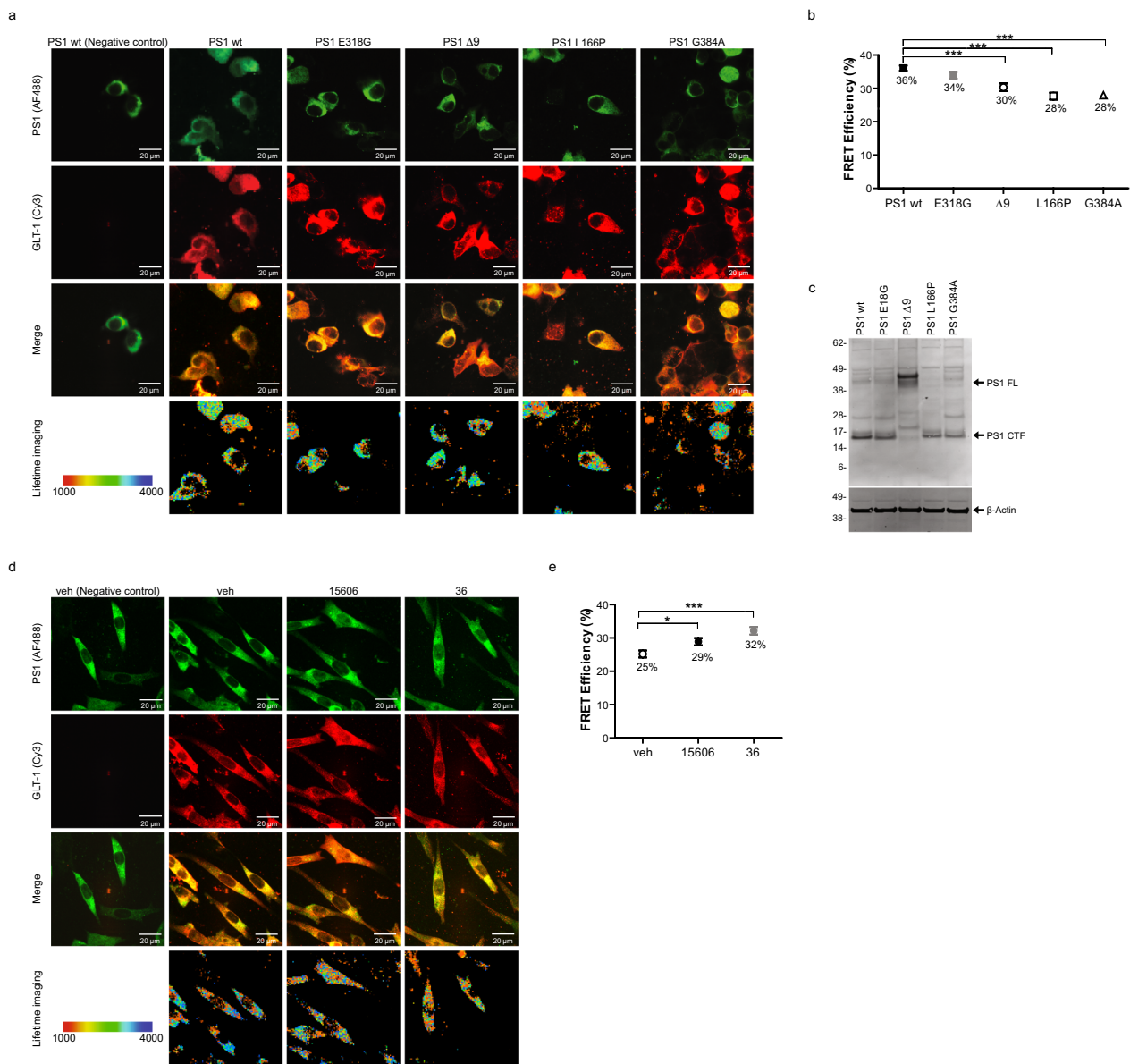
Fig. 2 PS1 conformation impacts the PS1/GLT-1 interaction. **a, b** Pathogenic fAD PS1 mutations decrease the PS1/GLT-1 interaction. HEK PS DKO cells transiently co-transfected with GLT-1 and wildtype PS1 or PS1 with familial AD mutations. **a** Confocal images of HEK PS DKO cells co-transfected with GLT-1 and PS1 and immunostained with anti-PS1 and anti-GLT-1 antibodies (top three panels). Bottom panel shows color-coded FLIM images of the donor fluorophore lifetimes in the cell. Orange-red pixels, corresponding to the shorter fluorescence lifetimes, are indicative of the closest proximity between the fluorophore-labeled PS1 and GLT-1. The colorimetric scale shows AF488 fluorescence lifetime in picoseconds. **b** FLIM analysis of the PS1/GLT-1 proximity (%EFRET) in cells expressing PS1 wildtype, non-pathogenic E318G, and fAD Δ9, L166P or G384A mutants with GLT-1 (3 independent replications, n = 108–112 cells per group). Error bars show ± SEM, ***$p < 0.001$. One-way ANOVA with Bonferroni's post-hoc correction. **c** Western blot representing the level of PS1 wt and PS1 fAD in presence of GLT-1. HEK PS DKO have been co-transfected with GLT-1 and PS1 wt or non-pathogenic E318G, or fAD Δ9, L166P or G384A mutants. **d, e** FLIM analysis of the PS1/GLT-1 proximity in CHO cells treated with PS1 conformation modifying gamma-secretase modulators (GSMs) reveals stronger FRET efficiency (%EFRET). (d) Top panels show cells transiently transfected with wildtype PS1 and GLT-1 DNA, and immunostained with anti-PS1 and anti-GLT-1 antibodies. Bottom panel shows color-coded FLIM images of the donor fluorophore lifetimes in the cell. Orange-red pixels, corresponding to the shorter fluorescence lifetimes, are indicative of the closest proximity between the fluorophore-labeled PS1 and GLT-1. The colorimetric scale shows AF488 fluorescence lifetime in picoseconds. (d) FLIM analysis (%EFRET) of GSM15606, GSM36, or vehicle control treated cells (4 independent replications, n = 108–112 cells per group). Error bars show ± SEM, *$p < 0.05$, ***$p < 0.001$. One-way ANOVA with Bonferroni's post-hoc correction

Perrin *et al. Acta Neuropathologica Communications*   (2024) 12:166

Page 8 of 17

High-resolution FLIM generated a color-coded image of the AF488 donor fluorophore lifetimes within each cell, reflecting proximity between the PS1 and GLT-1 (Fig. 2a bottom panel). We found that all fAD PS1 mutations tested decreased the PS1/GLT-1 interaction, measured by a decrease in FRET efficiency (Fig. 2b; one-way ANOVA with Bonferroni's *post-hoc* correction). Interestingly, in cells expressing non-pathogenic mutation E318G, the interaction between PS1 and GLT-1 did not differ from that in cells expressing wildtype PS1.

Next, we tested if altering PS1's conformation to be more open and non-pathogenic would impact the protein binding to GLT-1. We used GSM15606 and GSM36 to induce more "relaxed" PS1 conformations in CHO cells transiently co-transfected with GLT-1 stained with Cy3 and wildtype PS1 stained with AF488 (Fig. 2d). GSM treatment with either GSM15606 or GSM36 increased the PS1/GLT-1 interaction, measured by an increase in FRET efficiency, compared to vehicle treated cells (Fig. 2e; one-way ANOVA with Bonferroni's *post-hoc* correction). These results indicate that PS1

conformation and possibly its structural arrangement may be important for the binding of PS1 to GLT-1.

PS1 increases GLT-1 cell surface expression and multimerization

To determine if PS1 and its binding to GLT-1 may impact GLT-1 expression at the outer surface of the plasma membrane, where functional GLT-1 resides [1] we employed two complementary approaches. HEK PS DKO cells lacking both, PS1 and PS2 were transiently co-transfected with GLT-1 and PS1 or GLT-1 and pcDNA3.1-GFP vector (pc). Transfection of the HEK PS DKO cells with pcDNA3.1-GFP alone was used as a negative control. Intact cells were biotinylated to label the cell surface proteins, lysed, and biotin-tagged proteins were pulled down with Streptavidin. Western blotting with GLT-1 antibody detection was used to measure the effect of the presence of PS1 on GLT-1 levels at the cell surface. The amount of cell surface (biotinylated) GLT-1 protein was normalized to the level of cell surface EGFR in the same sample. We found increased GLT-1 cell surface expression in the presence of PS1 compared to that in pc control (Fig. 3a-b).
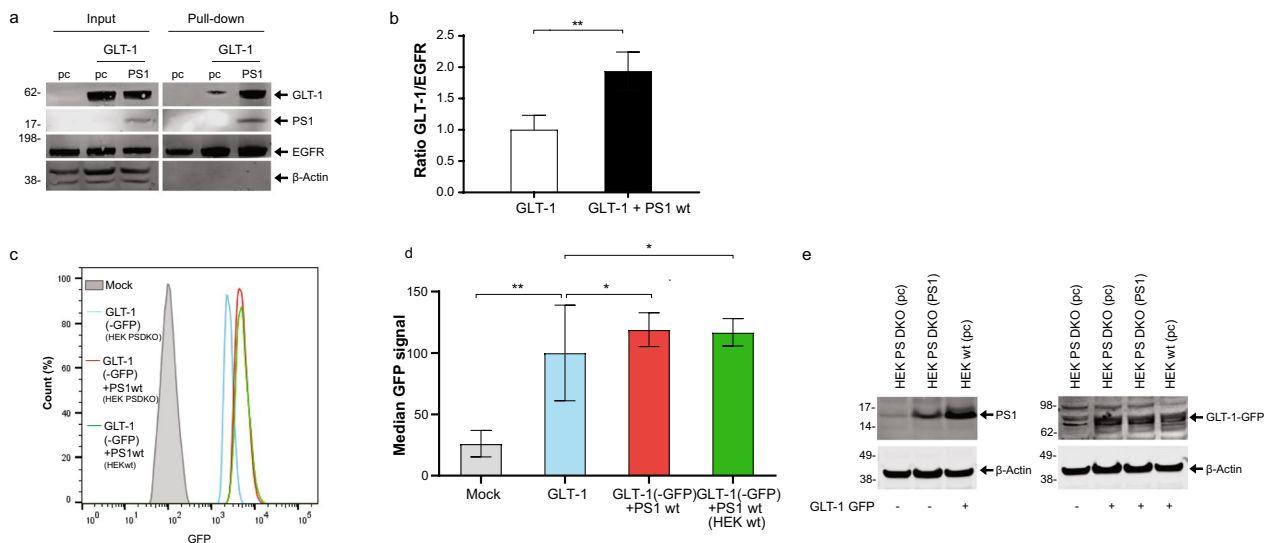

Fig. 3 PS1 increases GLT-1 cell surface expression **a** Representative western blots showing GLT-1 and PS1 total expression (input) and cell surface expression (Pull-down) in HEK PS DKO cells co-transfected with GLT-1 and either pcDNA3.1-PS1 or pcDNA3.1-GFP (pc). Left lane (pc) shows HEK PS DKO cells transfected with pc alone. The cells were biotinylated, lysed, and streptavidin was used for pull-down. Membranes were probed for GLT-1, PS1 CTF, EGFRand β-actin. **b** The presence of PS1 increases GLT-1 cell surface expression compared to GLT-1 in pcDNA3.1-GFP (pc) transfected cells. Biotinylation band intensity was equalized to cell surface EGFR, and normalized to GLT-1+pc in the input. Four independent replications per group, bars show mean±SEM. One-way ANOVA with Bonferroni's post-hoc correction. **$p < 0.01$. **c** Representative Flow cytometry analysis of GLT-1 cell surface in HEK cells. HEK PS DKO stably expressing GLT-1 GFP were transfected with pcDNA3.1 (in blue) or PS1wt (in red). Naïve HEKwt cells stably expressing GLT-1 GFP and PS1 at endogenous level are shown (in green). Mock (in grey) represents pcDNA3.1 empty vector transduced cells. Cells were analyzed alive and gated in regard to GLT-1-GFP signal. **d** Analysis of the median cell surface GFP signal was normalized to total GLT-1-GFP. N=3 independents experiments. bars show mean±SEM. One-way ANOVA with Bonferroni's post-hoc correction. *$p < 0.05$, **$p < 0.01$. **e** Representative western blots showing GLT-1-GFP and PS1 expression in HEK PS DKO and HEK wt cells used for Flow cytometry. The blot on the left compares the expression level of PS1 transiently transfected in HEK PS DKO vs the level of endogenous PS1 in HEK wt. The right blot compares the expression level of stably transduced GLT-1 GFP (+) in HEK PS DKO, with or without PS1 vs. HEK wt cell line

We have also used an alternative approach, flow cytometry, to examine the effect of PS1 on cell surface GLT-1 in HEK cells stably expressing GLT-1 GFP. HEK PS DKO cells were transfected with either pcDNA3.1 or PS1 (blue and red graphs in Fig. 3 c,d, e). HEK wt cells (green in Fig. 3 c,d) were used to verify that endogenously expressed PS1 would also affect the cell surface levels of GLT-1 when compared to HEK PS DKO GLT-1 GFP cells (blue in Fig. 3 c.d). Western blot analysis showed that stable GLT-1-GFP is expressed at comparable levels in HEK wt and in HEK PS DKO cell lines (Fig. 3e). The level of PS1 endogenously expressed in HEK wt or transiently transfected into HEK PS DKO is shown in Fig. 3e, left. We have also confirmed these results in CHO cells transiently co-transfected with GLT-1 and pcDNA3.1 or with GLT-1 and PS1 (Figure S4). The cells were fixed and stained with GLT-1 antibody without permeabilization, followed by PE-conjugated secondary antibody. Cells transfected with pcDNA3.1 empty vector (Mock) were labeled with IgG from rabbit as isotype negative control. The relative fluorescence intensity at the membrane surface of CHO expressing GLT-1-PS1 was increased in comparison to CHO cells expressing GLT-1 alone (Fig. S4a-b). The western blot analysis shows comparable levels of total GLT-1 expression in CHO cells with and without transfected PS1 (Fig. S4c). All flow cytometry experiments have shown similar results: more GLT-1 (GFP or PE labeled) appear at the cell surface in the presence of either endogenously or transiently expressed PS1, as compared to cells expressing GLT-1 alone.

Based on both biotinylation and flow cytometry assays, we can conclude that the presence of PS1 facilitates GLT-1 cell surface delivery.

GLT-1 multimerization occurs during the transporter maturation and is required for the transporter functional activity [25, 30, 80]. GLT-1 multimerization profile has been verified in human brain tissue. Human brain lysates, Control vs AD cases, were ran in non-denaturing condition using Native Blue Page (NB) assay (Fig. 4a). Interestingly, we observed that AD cases presented more PS1/ γ-secretase (Fig. 4a, right), and increase in GLT-1 dimer (~ 160 kDa) and trimer (~ 242 kDa) (Fig. 4a center, bottom image) but also more GLT-1 aggregates that are present above 480 kDa (Fig. 4a, left and center images). Increased ratio of the GLT-1 trimers over PS1/γ-secretase in AD brain (Fig. 4b) suggests that increased levels of PS1 and decreased interaction with GLT-1. To determine whether PS1 could alter homomultimerization of GLT-1 we have studied GLT-1 profile in HEK PS DKO cells after transient transfection of pcDNA3.1 GFP (pc) or co-transfection of GLT-1 with either pc or wildtype PS1 in non-denaturing condition. After probing with GLT-1 antibody we observed bands at around 70 kDa, 160 kDa

and 242 kDa corresponding to monomer, dimer and trimer, respectively (Fig. 4b). We have quantified the signal of monomer/dimer/trimer (total GLT-1 expression) and determined the relative intensity of each band as a percentage (Fig. 4c). In the absence of PS1, the amount of GLT-1 multimers, the functional form of GLT-1, represented 89.7% of the total GLT-1 expression. When GLT-1 is co-expressed with PS1, the GLT-1 multimers increased to 95.6% of the total GLT-1 expression. The increase of the GLT-1 homomultimers, especially functionally active trimers, relative to the level of GLT-1 monomers in the presence of PS1 was statistically significant (Fig. 4c; Two-way ANOVA with Sidak's multiple comparisons test). To verify further if GLT-1 multimerization profile is affected by PS1 we used a different approach – Western blotting in denaturing conditions after treating living cells with disuccinimidyl suberate (DSS) (+) to stabilize GLT-1 homomultimers (Fig. 4d). Cells were also treated with DMSO only (-) to confirm the multimers observed came from the DSS stabilization. Cells were lysed in 1% NP-40 + 0.1% Triton-X and resolved by SDS-PAGE. Trimers were only observed in the presence of DSS treatment. The GLT-1 monomer/dimer/trimer bands in DSS treated cells with and without PS1 were quantified after immunoblotting with GLT-1 antibody. We found that when GLT-1 is co-expressed with PS1, the percentage of GLT-1 monomer level slightly decreased, while the dimer and trimer sum correspondingly increased. The increase in the fraction of GLT-1 homomultimers (dimer + trimer) in the presence of PS1 was statistically significant as compared to that in cells without PS1 (Fig. 4e; Two-way ANOVA with Sidak's multiple comparisons test).

PS1 does not impact GLT-1 stability

To determine if the effect of PS1 on increased GLT-1 cell surface expression was due to an increase in GLT-1 protein stability, a cycloheximide chase assay was performed with HEK PS DKO cells transiently co-transfected with GLT-1 and either an empty pcDNA-GFP vector (pc) or wildtype PS1. pcDNA3.1-GFP was chosen as an "irrelevant protein" control. The decrease in GLT-1 protein was measured over the course of two days at various timepoints using Western blotting with GLT-1 antibody detection. PS1 did not significantly impact GLT-1's protein stability (Fig. 5a-b). Similar results were observed in CHO cells (Figure S5a-b).

PS1 modulate glutamate uptake mediated by GLT-1 after 10 min glutamate treatment

To determine if PS1 can modify GLT-1 glutamate uptake, we compared uptake of [^{3}H]-L-glutamate into HEK PS DKO cells stably expressing GLT-1 GFP (HEK PS DKO GLT-1) and transfected either with PS1 wt or pcDNA3.1
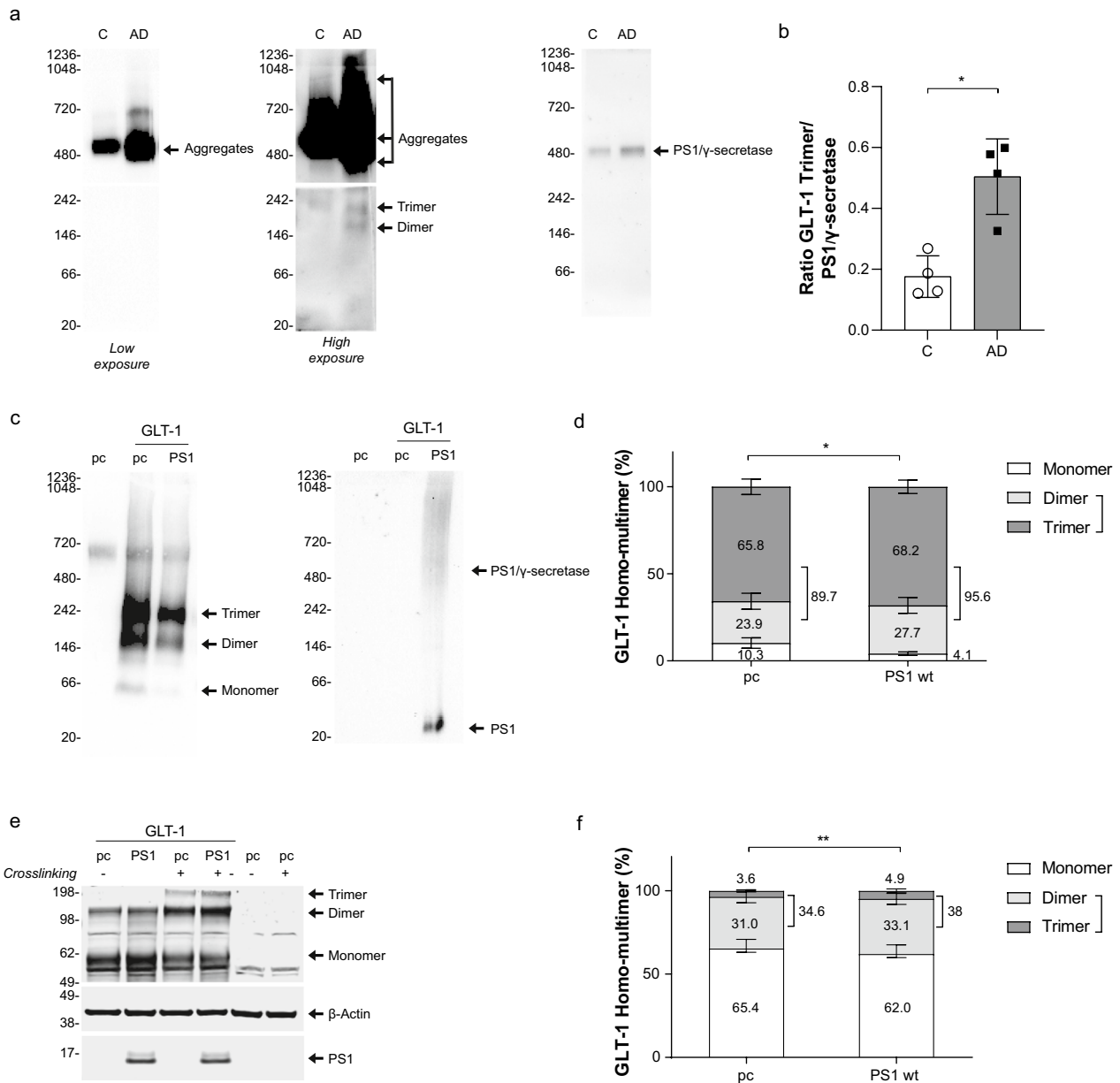
Fig. 4 PS1 induces GLT-1 multimerization **a** Representative immuno-blot after Blue Native Polyacrylamide Gel Electrophoresis (BN/PAGE) showing GLT-1 expression profile in Control vs AD human brain lysates (n = 4 for each group). First lane corresponds to control (C) and second lane Alzheimer's disease case (AD). The first two blots are probed with GLT-1 antibodies (Abcam); Intense bands are detected above 480 kDa and corresponding to GLT-1 aggregates. On high exposure blot, above 146 kDa and 242 kDa bands correspond to dimer and trimer respectively. Third blot is probed for PS1 (BioLegend) and shows PS1/γ-secretase complex. **b** Ratio of the GLT-1 trimer signal over PS1/γ-secretase complex. Bars show mean ± SD. N = 4 Control vs AD human brain lysates in each group. *p = 0.0286. T-test with Mann Whitney comparisons test. **c** Representative immuno-blot after BN/PAGE showing GLT-1 expression profile co-expressed with pcDNA3.1 (pc) or PS1. First lane corresponds to HEK PS DKO cells transfected with "pc" only. HEK PS DKO cells were treated with 5% digitonin prior BN/PAGE and Western blotting for GLT-1 detection. GLT-1 antibodies indicate 70 kDa, ~ 146 kDa and 242 kDa bands corresponding to monomer, dimer and trimer respectively. Second blot is probed for PS1 (BioLegend) and shows PS1/γ-secretase complex and PS1. **d** Quantification of relative intensity of GLT-1 monomer, dimer and trimer in absence (pc) or presence of PS1. The level of multimerization profile is measured in comparison of monomer vs dimer + trimer. Bars show mean ± SEM. N = 3 independent experiments in triplicates. *p < 0.0231. Two-way ANOVA with Sidak's multiple comparisons test. **e** Representative Western blots of HEK PS DKO cells, transiently transfected with GLT-1 and empty DNA vector (pc), or wildtype PS1. Cross-linking agent, DSS (disuccinimidyl suberate) (+), was used at 50 µM to stabilize GLT-1 multimers. (-) corresponds to cells treated with DMSO only. Membranes were probed for GLT-1, PS1 and β-actin as a loading control. GLT-1 antibody revealed 55 kDa, 120 kDa and 190 kDa bands corresponding to monomer, dimer and trimer respectively. **f** Quantification of the relative intensity of GLT-1 monomer, dimer and trimer bands crosslinked (Image Studio Lite). N = 6 independent experiments, bars show mean ± SEM, **p < 0.01. Two-way ANOVA with Sidak's multiple comparisons test
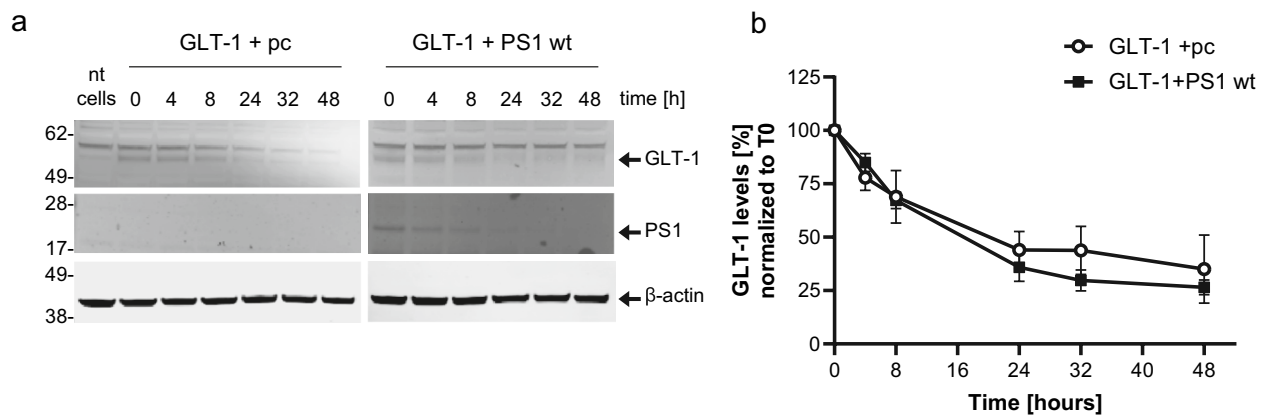
Fig. 5 PS1 does not impact GLT-1 protein stability. **a** Representative western blots of HEK PS DKO cells transiently transfected with GLT-1 and wildtype PS1 or pcDNA-GFP vector (pc) treated with cycloheximide (CHX) and lysed at various time points to determine relative GLT-1 protein stability. **b** PS1 did not significantly impact GLT-1's protein stability, as measured by the decrease of GLT-1 protein over time after treatment with CHX. 5 independent replications per group, bars show mean ± SEM. Two-way ANOVA followed by Dunnett's multiple comparisons

(pc) after five and ten minutes of the treatment. Glutamate uptake by the plasma membrane glutamate transporters is highly sodium dependent [79], and we determined the sodium dependent component of glutamate uptake in these experiments by measuring uptake in a sodium containing uptake buffer or in an uptake buffer in which sodium chloride was replaced by choline chloride. Total radioactive and non-radioactive glutamate was present at a concentration of 50 µM. The effect of GLT-1 inhibitors DHK (1 mM) or WAY213613 (10 µM) was assessed in cells assayed in parallel with cells not treated with inhibitors to verify that uptake was mediated by GLT-1 (Fig. 6a). Transport activity was inhibited by specific inhibitors of GLT-1. There was no significant difference in the glutamate uptake between genotypes at a 5-min time point. After longer, 10-min treatment, however, the uptake of glutamate increased significantly in the presence of PS1 compared to cells lacking PS1. To confirm PS1 expression in cells used for the GLT-1 glutamate uptake assay, we performed a Western blot analysis of the cell lysates (Fig. 6b).

GLT-1 interacts with PS2
PS1 and PS2 are highly homologous polytopic membrane proteins. Since we discovered that GLT-1 interacts with PS1, we next explored if GLT-1 may also bind to PS2. First, to ensure PS1 does not interfere with the coimmunoprecipitation, we used HEK PS DKO transiently co-transfected with GLT-1 and either PS2 wt or pcDNA 3.1. IgG was used as a negative control for immunoprecipitation. Western blot analysis of HEK PS DKO using the anti-PS2 C-terminal antibody for detection demonstrated the presence of a PS2-CTF band in the GLT-1 immunoprecipitated fraction (Figure S6a), suggesting

that the binding between the GLT-1 and PS2 may also occur.

To verify the GLT-1/PS2 interaction at endogenous level, we used primary neurons and mouse brain lysates. Endogenous GLT-1/PS2 complexes were detected by co-immunoprecipitation in neurons in vitro and in mouse brain tissue (Figure S6b and c, respectively). In addition, we confirmed the GLT-1/PS2 interaction by an alternative approach, FLIM analysis in intact neurons (Figure S6d). The median lifetime of AF488 (FRET donor) in neurons with AF488 labeled PS2 only is 2528 ± 290.1 ps, while AF488/PS2 lifetime in cells co-immunostained with Cy3/GLT-1 shortened to 2247 ± 172.8 ps. Shortening of the donor fluorophore lifetime indicates FRET signal, and thus close proximity between AF488/PS2 and Cy3/GLT-1.

Discussion
We recently found that PS1 and GLT-1 interact in the mouse brain, and this interaction occurs in both astrocytes and neurons cultured in vitro [81]. In the current study, we first established that PS1/GLT-1 interaction also occurs in the human brain. Interestingly, this interaction diminishes in the brain of sporadic AD patients compared to non-demented controls, as measured by FRET-based approach in intact tissue. Further, we compared PS1/GLT-1 interaction in sAD to FTLD, another dementia/neurodegeneration condition. FTLD may or may not have tau inclusions (NFT in Table 1), but unlike sAD, does not have amyloid pathology. Intriguingly, PS1/GLT-1 interaction was not significantly altered in FTLD brain and was comparable to that of controls. This indicates the specificity of diminished PS1/GLT-1 interaction to sAD and to amyloid pathology, by extension.
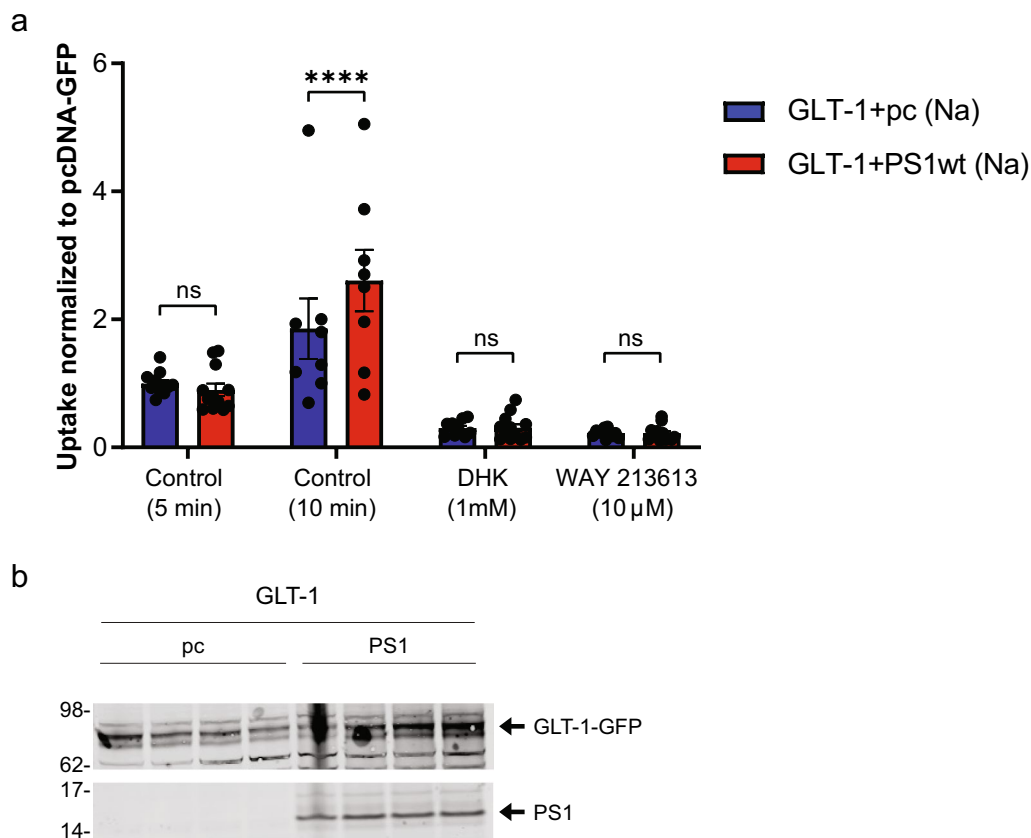
Fig. 6 PS1 alters GLT-1 mediated glutamate uptake in HEK cells after 10 min glutamate treatment. **a** [^{3}H]-L-glutamate uptake was assayed in HEK PS DKO cells stably expressing GLT-1. Cells were transfected with PS1 or control vector (see methods). Two days after transfection, experiment was performed in which cells were exposed to [^{3}H]-L-glutamate in a total glutamate concentration of 50 µM for 5 and 10 min at 37 °C. There were four groups of cells, two in which the GLT-1 specific inhibitors DHK (1 mM) or WAY213613 (10 uM) were present, and two others in which vehicle only was present. Four separate experiments were performed, each representing a separate passage and plating of the HEK cells, and the results shown are data pooled from those 4 experiments. Results are all normalized to the control (vehicle only) value from the PS1 negative (pc DNA-GFP) condition at 5 min. Error bars show SEM, ****$p < 0.0001$. Two-Way ANOVA mixed-effects analysis with Sidak's multiple comparisons test **b** Western blot of cell lysate used for GLT-1 glutamate uptake. Cell cultures for Western blotting were not exposed to [3H]-L-glutamate but were treated with sodium only, and the assay was performed in parallel with the glutamate uptake experiments. Membrane was probe with GLT-1 (ABCAM) antibody and PS1 antibody (CST)

PS1 adopts pathogenic "closed" conformation due to fAD PS1 mutations and in sAD, but not in FTLD brains [5, 67, 72]. Thus, we investigated the hypothesis that PS1 conformation disrupts PS1/GLT-1 interaction in sAD brain. For this, we used two complementary approaches known to affect PS1 conformation: fAD PS1 mutations, which induce a "closed" pathogenic conformation, and γ-secretase modulators, GSMs, which induce an "open" conformation [58, 67]. Our findings indicate that PS1 conformation has a direct effect on PS1/GLT-1 interaction, with fAD mutations reducing the interaction, and GSM treatment increasing the interaction. Of note, non-pathogenic PS1 E318G mutation, which does not change PS1 conformation [5], did not significantly alter PS1/GLT-1 interaction.

This suggests PS1/GLT-1 interaction is dynamically regulated by PS1 conformation, and changes in PS1 conformation due to aging, oxidative stress [2], or fAD mutations [5, 72] disrupt the structural arrangement of PS1 binding to GLT-1. Importantly, pathogenic changes in PS1, that result in a decrease in the PS1/GLT-1 interaction in AD, support the idea that this interaction may be beneficial. Plausibly, gradual and continued reduction in PS1/GLT-1 interaction occurring in AD brain, disrupts the localization or maturation of this glutamate transporter, as suggested by our in vitro data. This would help explain the strong association between fAD PS1 mutations and epileptiform activity [37] and more generally the hyperactivity of neural circuits observed in both fAD and sAD [7, 49, 57].

Perrin *et al. Acta Neuropathologica Communications*   (2024) 12:166

Page 13 of 17

The age, sex, Braak stage of the sAD cases, or PMI of the samples studied did not significantly affect PS1/GLT-1 interaction as measured by the FLIM assay. Regarding the ApoE genotype of the subjects, six of the eight AD cases used herein, with known ApoE, present at least one ApoE4 allele, whereas only one out of five FTLD cases was ApoE4 positive and all three C with known ApoE status were ApoE 3/3 (Supplementary Table 1). Therefore, we cannot exclude the possibility that ApoE may modulate PS1/GLT-1 interaction in direct or indirect manner by, for example, inducing a PS1 conformational change. While the ApoE status is unknown for most of the FTLD and C cases, the study by Hou et al. [26] provides valuable insights into the interaction between ApoE and γ-secretase, showing that ApoE can act as a substrate-specific inhibitor of γ-secretase, with the inhibitory potency varying across ApoE isoforms.

The reported data on the levels of GLT-1 protein in human brain are somewhat controversial, even for those studies that investigated the same brain regions [75]. Previous studies found no change in GLT-1 protein levels in the human frontal cortex [18] as well as the medial prefrontal cortex in an AD mouse model [33], whereas other research has described significant decrease in GLT-1 expression in the frontal cortex of AD patients [40] as well as a decrease in GLT-1 gene and protein expression in the hippocampus of sAD patients [28]. It was also reported, that GLT-1 aggregates are elevated in AD brains [74], and that oxidation damage to GLT-1, including oxidation damage as a result of exposure to Aβ [22, 31, 38], results in high-molecular weight GLT-1 oligomers [66]. Our findings agree with the findings of Woltjer et al. [74], and show significantly higher levels of GLT-1 aggregates in sAD brain, as detected by Native Blue PAGE assay. Detergent-soluble GLT-1 levels were reduced in AD compared to control brains, suggesting that GLT-1 may be a protein that exhibits altered solubility in AD. This change in GLT-1 solubility and expression may explain the conflicting results surrounding GLT-1 levels in the AD brain.

We found that control brains, besides aggregates, contained mainly GLT-1 trimers (functional form [21, 25, 78]), whereas AD brains also had significant amount of less mature GLT-1 dimers. In addition, we observed that PS1/γ-secretase complexes increase in AD human brain tissue compared to control cases, while transcriptomic analysis shows no impact on mRNA level [68]. This observation suggests, along with pathogenic "closed" PS1 conformation that prevents efficient binding to GLT-1, PS1 may misfold/accumulate in AD brain and cannot provide proper chaperoning activity leading to GLT-1' mislocalization and increased aggregation.

An important consideration is whether the interaction is relevant when it happens in astrocytes, neurons, or both. Although high levels of mRNA is detected in neurons [6, 56], GLT-1 protein is expressed more abundantly on astrocytes than on neurons and historically has been treated as primarily an astrocytic transporter [10, 39]. However, more recently GLT-1 has been found to have an impactful role in neurons that is disproportionate to its expression [44, 53, 59]. In vivo, neuronal GLT-1 primarily localizes to axons and synapses [17]; however, low levels of GLT-1 protein can be detected in cell bodies of some, presumably stressed neurons in the brain [54, 65]. We previously detected PS1/GLT-1 interaction in mouse primary astrocytes and primary neurons [81], and the current study detected this interaction in human tissue in both the parenchyma (GLT-1-positive astrocytes and axons) and in occasional neuronal cell bodies. Therefore, considering these results, we can conclude that this interaction occurs in both neurons and astrocytes but not if this interaction differs significantly between the two cell types pertinent to regulatory and functional consequences.

GLT-1 activity is regulated at multiple levels, including total protein expression, trafficking to the cell surface, and multimer formation [1]. To determine if PS1/GLT-1 interaction may influence GLT-1 localization at the cell surface, and therefore could indicate changes in GLT-1 maturation and function, we measured the effect of PS1 on GLT-1 cell surface expression, homomultimerization, stability, and glutamate uptake. At the cellular level, we found that the presence of PS1 increased GLT-1 multimer formation and GLT-1 cell surface expression. Our findings indicate that these changes were not due to an alteration in GLT-1 stability, as the presence of PS1 did not noticeably impact GLT-1 protein stability.

An important question that arises from this finding is whether changes in PS1/GLT-1 interaction result in a direct measurable modification of GLT-1 function. The challenge with experiments aimed to address this question is that synaptic dysfunction due to glutamate transport impairments in AD brain occurs chronically, over many years, possibly decades, whereas the current models of glutamate uptake report more acute changes. Our in vitro data suggest that PS1 directly interacting with GLT-1 may act as a chaperone for GLT-1, promoting or stabilizing its homo-multimerization and cell surface delivery, and potentially modulating GLT-1-mediated glutamate uptake, over time. We observed significant difference in the glutamate uptake between HEK PS DKO cells lacking PS1/PS2 and HEK PS DKO cells transiently transfected with human PS1, as assayed by measuring ^{3}H-L-glutamate uptake after 10-min treatment with glutamate. Given that PS1/GLT-1 interaction is reduced in

sAD brain leading to GLT-1 aggregation, it is possible, that it also impairs GLT1 cell surface trafficking in AD. This would have functional implication on glutamate uptake, and thus play a key role in excitotoxicity and neurodegeneration. Indeed, abnormal glutamate transport and hyperactivity have been reported as early events in AD, with high incidence of epileptic seizures in presymptomatic fAD mutations carriers [7, 42, 57, 70]. Furthermore, this study may provide a mechanistic insight into the previous findings that AD patients with PS1 mutations have significantly higher epileptiform activity [37, 49, 70]. Relevantly, the presence of Aβ disrupts glutamate transmission at the synapse and reduces local GLT-1 expression [13, 27, 61, 74]. Aβ-containing AD brain extracts can induce neuronal hyperactivity [82]. A recent transcriptomic study using human AD tissue has shown that hyperactivity is a prelude to a subsequent excitatory neuronal loss in their Aβ positive samples, and this cell state is specific to early AD pathology [19]. In AD mouse models, GLT-1 upregulation rescued cognitive decline [83] and GLT-1 loss increased cognitive decline [47], suggesting treating GLT-1 dysregulation might alleviate cognitive deficits observed in AD. In this scenario, a pathogenic conformational change in PS1 leads it to act as a faulty chaperone, failing to properly bind to and aid GLT-1 to reach the cell surface and/or to induce GLT-1 multimerization, which would compromise GLT-1 function.

Moreover, there could be other consequences of disrupted PS1/GLT1 interaction in sAD brain. For example, the synaptic protein PICK1 interacts with the isoform GLT-1b [3]. Subsequently, it was found that co-expression of PICK1 with GLT-1b in oocytes induced a substantial leak current mediated by GLT-1b [62]. GLT-1 expressed in astrocytes [20] and neurons [44, 45] has important metabolic functions, and metabolic consequences of the PS1/GLT1 interaction might not be discernible unless specifically looked for.

Conclusion
In conclusion, the current study establishes PS1/GLT-1 interaction occurs in the human brain and is disrupted in sAD, but not in FTLD. Additionally, the interaction may be important for GLT-1 multimerization and cell surface expression, and this interaction is dynamically regulated by PS1 conformation. Therefore, disruption of PS1/GLT-1 interaction due to PS1 conformational changes, either in fAD or sAD, could be a cause of impaired GLT-1 function and ultimately glutamate dyshomeostasis, providing a mechanistic link between glutamate transporter dysfunction and amyloid pathology. Thus, targeting PS1/GLT-1 interaction can be a potential new strategy for therapeutic intervention in AD.

Abbreviations

AD	Alzheimer's disease
ANOVA	One-way analysis of variance
Aβ	Amyloid β-protein
CHO	Chinese hamster ovary
DHK	Dihydrokainate
EAAT2	Excitatory amino acid transporter 2
fAD	Familial Alzheimer's disease
FLIM	FRET-based fluorescence lifetime imaging microscopy
FRET	Forster resonance energy transfer
FTLD	Frontotemporal lobar degeneration
GLT-1	Glutamate transporter 1
GSM	Gamma secretase modulator
HEK PS DKO	Human embryonic kidney presenilin double knock-out
ICC	Immunocytochemistry
IHC	Immunohistochemistry
NFT	Neurofibrillary tangle
PICK1	Protein interacting with C alpha kinase 1
PS1	Presenilin 1
sAD	Sporadic Alzheimer's disease

Supplementary Information

The online version contains supplementary material available at https://doi.org/10.1186/s40478-024-01876-y.

Additional file1 (PDF 1984 KB)

Additional file2 (PDF 347 KB)

Additional file3 (PDF 785 KB)

Additional file4 (PDF 522 KB)

Additional file5 (PDF 4404 KB)

Additional file6 (PDF 1257 KB)

Additional file7 (PDF 10682 KB)

Additional file8 (DOCX 20 KB)

Additional file9 (DOCX 21 KB)

Availability of data and material
All the uncropped blots are provided in Supplemental Fig. 7. All data generated or analyzed during this study are available upon demand.

Declarations

Ethics approval and consent to participate
Human tissue was provided by the Massachusetts Alzheimer's Disease Research Center (ADRC) with approval from the Mass General Brigham IRB (1999P009556).

References

1. Anderson CM, Swanson RA (2000) Astrocyte glutamate transport: review of properties, regulation, and physiological functions. Glia 32:1–14
2. Arimon M, Takeda S, Post KL, Svirsky S, Hyman BT, Berezovska O (2015) Oxidative stress and lipid peroxidation are upstream of amyloid pathology. Neurobiol Dis 84:109–119. https://doi.org/10.1016/j.nbd.2015.06.013
3. Bassan M, Liu H, Madsen KL, Armsen W, Zhou J, Desilva T, Chen W, Paradise A, Brasch MA, Staudinger J et al (2008) Interaction between the glutamate transporter GLT1b and the synaptic PDZ domain protein PICK1. Eur J Neurosci 27:66–82. https://doi.org/10.1111/j.1460-9568.2007.05986.x
4. Berezin MY, Achilefu S (2010) Fluorescence lifetime measurements and biological imaging. Chem Rev 110:2641–2684. https://doi.org/10.1021/cr900343z
5. Berezovska O, Lleo A, Herl LD, Frosch MP, Stern EA, Bacskai BJ, Hyman BT (2005) Familial Alzheimer's disease presenilin 1 mutations cause alterations in the conformation of presenilin and interactions with amyloid precursor protein. J Neurosci 25:3009–3017. https://doi.org/10.1523/jneurosci.0364-05.2005
6. Berger UV, Hediger MA (2001) Differential distribution of the glutamate transporters GLT-1 and GLAST in tanycytes of the third ventricle. J Comp Neurol 433:101–114. https://doi.org/10.1002/cne.1128
7. Bookheimer SY, Strojwas MH, Cohen MS, Saunders AM, Pericak-Vance MA, Mazziotta JC, Small GW (2000) Patterns of brain activation in people at risk for Alzheimer's disease. N Engl J Med 343:450–456. https://doi.org/10.1056/nejm200008173430701
8. Borchelt DR, Thinakaran G, Eckman CB, Lee MK, Davenport F, Ratovitsky T, Prada CM, Kim G, Seekins S, Yager D et al (1996) Familial Alzheimer's disease-linked presenilin 1 variants elevate Abeta1-42/1-40 ratio in vitro and in vivo. Neuron 17:1005–1013. https://doi.org/10.1016/s0896-6273(00)80230-5
9. Busche MA, Chen X, Henning HA, Reichwald J, Staufenbiel M, Sakmann B, Konnerth A (2012) Critical role of soluble amyloid-beta for early hippocampal hyperactivity in a mouse model of Alzheimer's disease. Proc Natl Acad Sci USA 109:8740–8745. https://doi.org/10.1073/pnas.1206171109
10. Chaudhry FA, Lehre KP, van Lookeren CM, Ottersen OP, Danbolt NC, Storm-Mathisen J (1995) Glutamate transporters in glial plasma membranes: highly differentiated localizations revealed by quantitative ultrastructural immunocytochemistry. Neuron 15:711–720. https://doi.org/10.1016/0896-6273(95)90158-2
11. Chen W, Aoki C, Mahadomrongkul V, Gruber CE, Wang GJ, Blitzblau R, Irwin N, Rosenberg PA (2002) Expression of a variant form of the glutamate transporter GLT1 in neuronal cultures and in neurons and astrocytes in the rat brain. J Neurosci : Off J Socfor Neurosci 22:2142–2152. https://doi.org/10.1523/JNEUROSCI.22-06-02142.2002
12. Chin J, Scharfman HE (2013) Shared cognitive and behavioral impairments in epilepsy and Alzheimer's disease and potential underlying mechanisms. Epilepsy Behavior : E&B 26:343–351. https://doi.org/10.1016/j.yebeh.2012.11.040
13. Danysz W, Parsons CG (1998) Glycine and N-methyl-D-aspartate receptors: physiological significance and possible therapeutic applications. Pharmacol Rev 50:597–664
14. De Strooper B, Annaert W, Cupers P, Saftig P, Craessaerts K, Mumm JS, Schroeter EH, Schrijvers V, Wolfe MS, Ray WJ et al (1999) A presenilin-1-dependent gamma-secretase-like protease mediates release of Notch intracellular domain. Nature 398:518–522. https://doi.org/10.1038/19083
15. Dickerson BC, Salat DH, Greve DN, Chua EF, Rand-Giovannetti E, Rentz DM, Bertram L, Mullin K, Tanzi RE, Blacker D et al (2005) Increased hippocampal activation in mild cognitive impairment compared to normal aging and AD. Neurology 65:404–411. https://doi.org/10.1212/01.wnl.0000171450.97464.49
16. Fan S, Xian X, Li L, Yao X, Hu Y, Zhang M, Li W (2018) ceftriaxone improves cognitive function and upregulates GLT-1-related glutamate-glutamine cycle in APP/PS1 mice. J Alzheimer's Disease : JAD 66:1731–1743. https://doi.org/10.3233/jad-180708
17. Furness DN, Dehnes Y, Akhtar AQ, Rossi DJ, Hamann M, Grutle NJ, Gundersen V, Holmseth S, Lehre KP, Ullensvang K et al (2008) A quantitative assessment of glutamate uptake into hippocampal synaptic terminals and astrocytes: new insights into a neuronal role for excitatory amino acid transporter 2 (EAAT2). Neuroscience 157:80–94. https://doi.org/10.1016/j.neuroscience.2008.08.043
18. Garcia-Esparcia P, Diaz-Lucena D, Ainciburu M, Torrejon-Escribano B, Carmona M, Llorens F, Ferrer I (2018) Glutamate transporter GLT1 expression in Alzheimer disease and dementia with Lewy bodies. Frontiers in aging neuroscience 10:122. https://doi.org/10.3389/fnagi.2018.00122
19. Gazestani V, Kamath T, Nadaf NM, Dougalis A, Burris SJ, Rooney B, Junkkari A, Vanderburg C, Pelkonen A, Gomez-Budia M et al (2023) Early Alzheimer's disease pathology in human cortex involves transient cell states. Cell 186(4438–4453):e4423. https://doi.org/10.1016/j.cell.2023.08.005
20. Genda EN, Jackson JG, Sheldon AL, Locke SF, Greco TM, O'Donnell JC, Spruce LA, Xiao R, Guo W, Putt M et al (2011) Co-compartmentalization of the astroglial glutamate transporter, GLT-1, with glycolytic enzymes and mitochondria. J Neurosci 31:18275–18288. https://doi.org/10.1523/JNEUROSCI.3305-11.2011
21. Gendreau S, Voswinkel S, Torres-Salazar D, Lang N, Heidtmann H, Detro-Dassen S, Schmalzing G, Hidalgo P, Fahlke C (2004) A trimeric quaternary structure is conserved in bacterial and human glutamate transporters. J Biol Chem 279:39505–39512. https://doi.org/10.1074/jbc.M408038200
22. Guo ZH, Mattson MP (2000) Neurotrophic factors protect cortical synaptic terminals against amyloid and oxidative stress-induced impairment of glucose transport, glutamate transport and mitochondrial function. Cerebral cortex(New York, NY : 1991) 10:50–57. https://doi.org/10.1093/cercor/10.1.50
23. Hamidi N, Nozad A, Sheikhkanloui Milan H, Salari AA, Amani M (2019) Effect of ceftriaxone on paired-pulse response and long-term potentiation of hippocampal dentate gyrus neurons in rats with Alzheimer-like disease. Life Sci 238:116969. https://doi.org/10.1016/j.lfs.2019.116969
24. Hascup KN, Hascup ER (2015) Altered neurotransmission prior to cognitive decline in AbetaPP/PS1 mice, a model of Alzheimer's disease. Journal of Alzheimer's disease : JAD 44:771–776. https://doi.org/10.3233/jad-142160
25. Haugeto O, Ullensvang K, Levy LM, Chaudhry FA, Honore T, Nielsen M, Lehre KP, Danbolt NC (1996) Brain glutamate transporter proteins form homomultimers. J Biol Chem 271:27715–27722. https://doi.org/10.1074/jbc.271.44.27715
26. Hou X, Zhang X, Zou H, Guan M, Fu C, Wang W, Zhang ZR, Geng Y, Chen Y (2023) Differential and substrate-specific inhibition of gamma-secretase by the C-terminal region of ApoE2, ApoE3, and ApoE4. Neuron 111(1898–1913):e1895. https://doi.org/10.1016/j.neuron.2023.03.024
27. Huang S, Tong H, Lei M, Zhou M, Guo W, Li G, Tang X, Li Z, Mo M, Zhang X et al (2018) Astrocytic glutamatergic transporters are involved in Abeta-induced synaptic dysfunction. Brain Res 1678:129–137. https://doi.org/10.1016/j.brainres.2017.10.011
28. Jacob CP, Koutsilieri E, Bartl J, Neuen-Jacob E, Arzberger T, Zander N, Ravid R, Roggendorf W, Riederer P, Grunblatt E (2007) Alterations in expression of glutamatergic transporters and receptors in sporadic Alzheimer's disease. J Alzheimer's Disease : JAD 11:97–116. https://doi.org/10.3233/jad-2007-11113
29. Joutsa J, Rinne JO, Karrasch M, Hermann B, Johansson J, Anttinen A, Eskola O, Helin S, Shinnar S, Sillanpaa M (2017) Brain glucose metabolism and its relation to amyloid load in middle-aged adults with childhood-onset epilepsy. Epilepsy Res 137:69–72. https://doi.org/10.1016/j.eplepsyres.2017.09.006
30. Kato T, Kusakizako T, Jin C, Zhou X, Ohgaki R, Quan L, Xu M, Okuda S, Kobayashi K, Yamashita K et al (2022) Structural insights into inhibitory mechanism of human excitatory amino acid transporter EAAT2. Nat Commun 13:4714. https://doi.org/10.1038/s41467-022-32442-6

Perrin *et al. Acta Neuropathologica Communications*   (2024) 12:166

Page 16 of 17

31. Keller JN, Pang Z, Geddes JW, Begley JG, Germeyer A, Waeg G, Mattson MP (1997) Impairment of glucose and glutamate transport and induction of mitochondrial oxidative stress and dysfunction in synaptosomes by amyloid beta-peptide: role of the lipid peroxidation product 4-hydroxynonenal. J Neurochem 69:273–284. https://doi.org/10.1046/j.1471-4159.1997.69010273.x

32. Kobayashi E, Nakano M, Kubota K, Himuro N, Mizoguchi S, Chikenji T, Otani M, Mizue Y, Nagaishi K, Fujimiya M (2018) Activated forms of astrocytes with higher GLT-1 expression are associated with cognitive normal subjects with Alzheimer pathology in human brain. Sci Rep 8:1712. https://doi.org/10.1038/s41598-018-19442-7

33. Kulijewicz-Nawrot M, Sykova E, Chvatal A, Verkhratsky A, Rodriguez JJ (2013) Astrocytes and glutamate homoeostasis in Alzheimer's disease: a decrease in glutamine synthetase, but not in glutamate transporter-1, in the prefrontal cortex. ASN Neuro 5:273–282. https://doi.org/10.1042/an20130017

34. Lakowicz JR (1999) Principles of fluorescence spectroscopy. Kluwer Academic/Plenum, City

35. Lakowicz JR, Szmacinski H, Nowaczyk K, Berndt KW, Johnson M (1992) Fluorescence lifetime imaging. Anal Biochem 202:316–330. https://doi.org/10.1016/0003-2697(92)90112-k

36. Lakowicz JR, Szmacinski H, Nowaczyk K, Lederer WJ, Kirby MS, Johnson ML (1994) Fluorescence lifetime imaging of intracellular calcium in COS cells using Quin-2. Cell Calcium 15:7–27. https://doi.org/10.1016/0143-4160(94)90010-7

37. Larner AJ (2011) Presenilin-1 mutation Alzheimer's disease: a genetic epilepsy syndrome? Epilepsy Behavior : E&B 21:20–22. https://doi.org/10.1016/j.yebeh.2011.03.022

38. Lauderback CM, Hackett JM, Huang FF, Keller JN, Szweda LI, Markesbery WR, Butterfield DA (2001) The glial glutamate transporter, GLT-1, is oxidatively modified by 4-hydroxy-2-nonenal in the Alzheimer's disease brain: the role of Abeta1-42. J Neurochem 78:413–416. https://doi.org/10.1046/j.1471-4159.2001.00451.x

39. Lehre KP, Levy LM, Ottersen OP, Storm-Mathisen J, Danbolt NC (1995) Differential expression of two glial glutamate transporters in the rat brain: quantitative and immunocytochemical observations. J Neurosci Off J Soc Neurosci 15:1835–1853. https://doi.org/10.1523/JNEUROSCI.15-03-01835.1995

40. Li S, Mallory M, Alford M, Tanaka S, Masliah E (1997) Glutamate transporter alterations in Alzheimer disease are possibly associated with abnormal APP expression. J Neuropathol Exp Neurol 56:901–911. https://doi.org/10.1097/00005072-199708000-00008

41. Lleo A, Berezovska O, Herl L, Raju S, Deng A, Bacskai BJ, Frosch MP, Irizarry M, Hyman BT (2004) Nonsteroidal anti-inflammatory drugs lower Abeta42 and change presenilin 1 conformation. Nat Med 10:1065–1066. https://doi.org/10.1038/nm1112

42. Masliah E, Alford M, DeTeresa R, Mallory M, Hansen L (1996) Deficient glutamate transport is associated with neurodegeneration in Alzheimer's disease. Ann Neurol 40:759–766. https://doi.org/10.1002/ana.410400512

43. Matos M, Augusto E, Oliveira CR, Agostinho P (2008) Amyloid-beta peptide decreases glutamate uptake in cultured astrocytes: involvement of oxidative stress and mitogen-activated protein kinase cascades. Neuroscience 156:898–910. https://doi.org/10.1016/j.neuroscience.2008.08.022

44. McNair LF, Andersen JV, Aldana BI, Hohnholt MC, Nissen JD, Sun Y, Fischer KD, Sonnewald U, Nyberg N, Webster SC et al (2019) Deletion of neuronal GLT-1 in mice reveals its role in synaptic glutamate homeostasis and mitochondrial function. J Neurosci 39:4847–4863. https://doi.org/10.1523/jneurosci.0894-18.2019

45. McNair LF, Andersen JV, Nissen JD, Sun Y, Fischer KD, Hodgson NW, Du M, Aoki CJ, Waagepetersen HS, Rosenberg PA et al (2020) Conditional knockout of GLT-1 in neurons leads to alterations in aspartate homeostasis and synaptic mitochondrial metabolism in striatum and hippocampus. Neurochem Res 45:1420–1437. https://doi.org/10.1007/s11064-020-03000-7

46. Mi DJ, Dixit S, Warner TA, Kennard JA, Scharf DA, Kessler ES, Moore LM, Consoli DC, Bown CW, Eugene AJ et al (2018) Altered glutamate clearance in ascorbate deficient mice increases seizure susceptibility and contributes to cognitive impairment in APP/PSEN1 mice. Neurobiol Aging 71:241–254. https://doi.org/10.1016/j.neurobiolaging.2018.08.002

47. Mookherjee P, Green PS, Watson GS, Marques MA, Tanaka K, Meeker KD, Meabon JS, Li N, Zhu P, Olson VG et al (2011) GLT-1 loss accelerates cognitive deficit onset in an Alzheimer's disease animal model. J of Alzheimer's Disease : JAD 26:447–455. https://doi.org/10.3233/jad-2011-110503

48. Pajarillo E, Rizor A, Lee J, Aschner M, Lee E (2019) The role of astrocytic glutamate transporters GLT-1 and GLAST in neurological disorders: potential targets for neurotherapeutics. Neuropharmacol 161:107559. https://doi.org/10.1016/j.neuropharm.2019.03.002

49. Palop JJ, Mucke L (2009) Epilepsy and cognitive impairments in Alzheimer disease. Arch Neurol 66:435–440. https://doi.org/10.1001/archneurol.2009.15

50. Palop JJ, Mucke L (2016) Network abnormalities and interneuron dysfunction in Alzheimer disease. Nat Rev Neurosci 17:777–792. https://doi.org/10.1038/nrn.2016.141

51. Perrin F, Sinha P, Mitchell SPC, Sadek M, Maesako M, Berezovska O (2024) Identification of PS1/gamma-secretase and glutamate transporter GLT-1 interaction sites. J Biol Chem 300:107172. https://doi.org/10.1016/j.jbc.2024.107172

52. Peterson AR, Binder DK (2019) Post-translational regulation of GLT-1 in neurological diseases and its potential as an effective therapeutic target. Front Mol Neurosci 12:164. https://doi.org/10.3389/fnmol.2019.00164

53. Petr GT, Sun Y, Frederick NM, Zhou Y, Dhamne SC, Hameed MQ, Miranda C, Bedoya EA, Fischer KD, Armsen W et al (2015) Conditional deletion of the glutamate transporter GLT-1 reveals that astrocytic GLT-1 protects against fatal epilepsy while neuronal GLT-1 contributes significantly to glutamate uptake into synaptosomes. J Neurosci 35:5187–5201. https://doi.org/10.1523/jneurosci.4255-14.2015

54. Pow DV, Cook DG (2009) Neuronal expression of splice variants of "glial" glutamate transporters in brains afflicted by Alzheimer's disease: unmasking an intrinsic neuronal property. Neurochem Res 34:1748–1757. https://doi.org/10.1007/s11064-009-9957-0

55. Prikhodko O, Rynearson KD, Sekhon T, Mante MM, Nguyen PD, Rissman RA, Tanzi RE, Wagner SL (2020) The GSM BPN-15606 as a potential candidate for preventative therapy in Alzheimer's disease. J Alzheimer's Disease : JAD 73:1541–1554. https://doi.org/10.3233/JAD-190442

56. Proper EA, Hoogland G, Kappen SM, Jansen GH, Rensen MG, Schrama LH, van Veelen CW, van Rijen PC, van Nieuwenhuizen O, Gispen WH et al (2002) Distribution of glutamate transporters in the hippocampus of patients with pharmaco-resistant temporal lobe epilepsy. Brain 125:32–43. https://doi.org/10.1093/brain/awf001

57. Quiroz YT, Budson AE, Celone K, Ruiz A, Newmark R, Castrillon G, Lopera F, Stern CE (2010) Hippocampal hyperactivation in presymptomatic familial Alzheimer's disease. Ann Neurol 68:865–875. https://doi.org/10.1002/ana.22105

58. Raven F, Ward JF, Zoltowska KM, Wan Y, Bylykbashi E, Miller SJ, Shen X, Choi SH, Rynearson KD, Berezovska O et al (2017) Soluble gamma-secretase modulators attenuate Alzheimer's beta-amyloid pathology and Induce conformational changes in presenilin 1. EBioMedicine 24:93–101. https://doi.org/10.1016/j.ebiom.2017.08.028

59. Rimmele TS, Rosenberg PA (2016) GLT-1: The elusive presynaptic glutamate transporter. Neurochem Int 98:19–28. https://doi.org/10.1016/j.neuint.2016.04.010

60. Rothstein JD, Dykes-Hoberg M, Pardo CA, Bristol LA, Jin L, Kuncl RW, Kanai Y, Hediger MA, Wang Y, Schielke JP et al (1996) Knockout of glutamate transporters reveals a major role for astroglial transport in excitotoxicity and clearance of glutamate. Neuron 16:675–686. https://doi.org/10.1016/s0896-6273(00)80086-0

61. Scimemi A, Meabon JS, Woltjer RL, Sullivan JM, Diamond JS, Cook DG (2013) Amyloid-beta1-42 slows clearance of synaptically released glutamate by mislocalizing astrocytic GLT-1. J Neurosc : Off J Soc Neurosci 33:5312–5318. https://doi.org/10.1523/jneurosci.5274-12.2013

62. Sogaard R, Borre L, Braunstein TH, Madsen KL, MacAulay N (2013) Functional modulation of the glutamate transporter variant GLT1b by the PDZ domain protein PICK1. J Biol Chem 288:20195–20207. https://doi.org/10.1074/jbc.M113.471128

63. Sperling RA, Laviolette PS, O'Keefe K, O'Brien J, Rentz DM, Pihlajamaki M, Marshall G, Hyman BT, Selkoe DJ, Hedden T et al (2009) Amyloid deposition is associated with impaired default network function in older persons without dementia. Neuron 63:178–188. https://doi.org/10.1016/j.neuron.2009.07.003

64. Tanaka K, Watase K, Manabe T, Yamada K, Watanabe M, Takahashi K, Iwama H, Nishikawa T, Ichihara N, Kikuchi T et al (1997) Epilepsy and

Perrin *et al. Acta Neuropathologica Communications*   (2024) 12:166

Page 17 of 17

exacerbation of brain injury in mice lacking the glutamate transporter GLT-1. Science (New York, NY) 276:1699–1702. https://doi.org/10.1126/science.276.5319.1699

65. Thal DR (2002) Excitatory amino acid transporter EAAT-2 in tangle-bearing Neurons in Alzheimer's disease. Brain Pathol 12:405–411. https://doi.org/10.1111/j.1750-3639.2002.tb00457.x

66. Trotti D, Rizzini BL, Rossi D, Haugeto O, Racagni G, Danbolt NC, Volterra A (1997) Neuronal and glial glutamate transporters possess an SH-based redox regulatory mechanism. Eur J Neurosci 9:1236–1243. https://doi.org/10.1111/j.1460-9568.1997.tb01478.x

67. Uemura K, Lill CM, Li X, Peters JA, Ivanov A, Fan Z, DeStrooper B, Bacskai BJ, Hyman BT, Berezovska O (2009) Allosteric modulation of PS1/gamma-secretase conformation correlates with amyloid beta(42/40) ratio. PLoS ONE 4:e7893. https://doi.org/10.1371/journal.pone.0007893

68. Viejo L, Noori A, Merrill E, Das S, Hyman BT, Serrano-Pozo A (2022) Systematic review of human post-mortem immunohistochemical studies and bioinformatics analyses unveil the complexity of astrocyte reaction in Alzheimer's disease. Neuropathol Appl Neurobiol 48:e12753. https://doi.org/10.1111/nan.12753

69. Voglein J, Noachtar S, McDade E, Quaid KA, Salloway S, Ghetti B, Noble J, Berman S, Chhatwal J, Mori H et al (2019) Seizures as an early symptom of autosomal dominant Alzheimer's disease. Neurobiol Aging 76:18–23. https://doi.org/10.1016/j.neurobiolaging.2018.11.022

70. Voglein J, Willem M, Trambauer J, Schonecker S, Dieterich M, Biskup S, Giudici C, Utz K, Oberstein T, Brendel M et al (2019) Identification of a rare presenilin 1 single amino acid deletion mutation (F175del) with unusual amyloid-beta processing effects. Neurobiol Aging 84(241):e245–e241. https://doi.org/10.1016/j.neurobiolaging.2019.08.034

71. Wagner SL, Zhang C, Cheng S, Nguyen P, Zhang X, Rynearson KD, Wang R, Li Y, Sisodia SS, Mobley WC et al (2014) Soluble gamma-secretase modulators selectively inhibit the production of the 42-amino acid amyloid beta peptide variant and augment the production of multiple carboxy-truncated amyloid beta species. Biochemistry 53:702–713. https://doi.org/10.1021/bi401537v

72. Wahlster L, Arimon M, Nasser-Ghodsi N, Post KL, Serrano-Pozo A, Uemura K, Berezovska O (2013) Presenilin-1 adopts pathogenic conformation in normal aging and in sporadic Alzheimer's disease. Acta Neuropathol 125:187–199. https://doi.org/10.1007/s00401-012-1065-6

73. Wolfe MS, Xia W, Ostaszewski BL, Diehl TS, Kimberly WT, Selkoe DJ (1999) Two transmembrane aspartates in presenilin-1 required for presenilin endoproteolysis and gamma-secretase activity. Nature 398:513–517. https://doi.org/10.1038/19077

74. Woltjer RL, Duerson K, Fullmer JM, Mookherjee P, Ryan AM, Montine TJ, Kaye JA, Quinn JF, Silbert L, Erten-Lyons D et al (2010) Aberrant detergent-insoluble excitatory amino acid transporter 2 accumulates in Alzheimer disease. J Neuropathol Exp Neurol 69:667–676. https://doi.org/10.1097/NEN.0b013e3181e24adb

75. Wood OWG, Yeung JHY, Faull RLM, Kwakowsky A (2022) EAAT2 as a therapeutic research target in Alzheimer's disease: a systematic review. Front Neurosci 16:952096. https://doi.org/10.3389/fnins.2022.952096

76. Xu M, Dong Y, Wan S, Yan T, Cao J, Wu L, Bi K, Jia Y (2016) Schisantherin B ameliorates Abeta1-42-induced cognitive decline via restoration of GLT-1 in a mouse model of Alzheimer's disease. Physiol Behav 167:265–273. https://doi.org/10.1016/j.physbeh.2016.09.018

77. Yang Y, Kinney GA, Spain WJ, Breitner JC, Cook DG (2004) Presenilin-1 and intracellular calcium stores regulate neuronal glutamate uptake. J Neurochem 88:1361–1372. https://doi.org/10.1046/j.1471-4159.2003.02279.x

78. Yernool D, Boudker O, Jin Y, Gouaux E (2004) Structure of a glutamate transporter homologue from pyrococcus horikoshii. Nature 431:811–818. https://doi.org/10.1038/nature03018

79. Zerangue N, Kavanaugh MP (1996) Flux coupling in a neuronal glutamate transporter. Nature 383:634–637

80. Zhang Z, Chen H, Geng Z, Yu Z, Li H, Dong Y, Zhang H, Huang Z, Jiang J, Zhao Y (2022) Structural basis of ligand binding modes of human EAAT2. Nat Commun 13:3329. https://doi.org/10.1038/s41467-022-31031-x

81. Zoltowska KM, Maesako M, Meier J, Berezovska O (2018) Novel interaction between Alzheimer's disease-related protein presenilin 1 and glutamate transporter 1. Sci Rep 8:8718. https://doi.org/10.1038/s41598-018-26888-2

82. Zott B, Simon MM, Hong W, Unger F, Chen-Engerer HJ, Frosch MP, Sakmann B, Walsh DM, Konnerth A (2019) A vicious cycle of beta amyloid-dependent neuronal hyperactivation. Science (New York, NY) 365:559–565. https://doi.org/10.1126/science.aay0198

83. Zumkehr J, Rodriguez-Ortiz CJ, Cheng D, Kieu Z, Wai T, Hawkins C, Kilian J, Lim SL, Medeiros R, Kitazawa M (2015) Ceftriaxone ameliorates tau pathology and cognitive decline via restoration of glial glutamate transporter in a mouse model of Alzheimer's disease. Neurobiol Aging 36:2260–2271. https://doi.org/10.1016/j.neurobiolaging.2015.04.005

Publisher's Note

Springer Nature remains neutral with regard to jurisdictional claims in published maps and institutional affiliations.